Dissipative Pairing Interactions: Quantum Instabilities, Topological Light, and Volume-Law Entanglement

Andrew Pocklington, Yu-Xin Wang, and A. A. Clerk

Phys. Rev. Lett. **130**, 123602 — Published 23 March 2023

DOI: 10.1103/PhysRevLett.130.123602

Dissipative Pairing Interactions: Quantum Instabilities, Topological Light, and Volume-Law Entanglement

Andrew Pocklington,[1,2] Yu-Xin Wang,[1] and A. A. Clerk[1]

[1] *Pritzker School of Molecular Engineering, University of Chicago, 5640 South Ellis Avenue, Chicago, Illinois 60637, U.S.A.*

[2] *Department of Physics, University of Chicago, 5640 South Ellis Avenue, Chicago, Illinois 60637, U.S.A.*

(Dated: January 25, 2023)

We analyze an unusual class of bosonic dynamical instabilities that arise from dissipative (or non-Hermitian) pairing interactions. We show that, surprisingly, a completely stable dissipative pairing interaction can be combined with simple hopping or beam-splitter interactions (also stable) to generate instabilities. Further, we find that the dissipative steady state in such a situation remains completely pure up until the instability threshold (in clear distinction from standard parametric instabilities). These pairing-induced instabilities also exhibit an extremely pronounced sensitivity to wavefunction localization. This provides a simple yet powerful method for selectively populating and entangling edge modes of photonic (or more general bosonic) lattices having a topological bandstructure. The underlying dissipative pairing interaction is experimentally resource-friendly, requiring the addition of a single additional localized interaction to an existing lattice, and is compatible with a number of existing platforms, including superconducting circuits.

Introduction.—Hamiltonian bosonic pairing interactions (where excitations are coherently created or destroyed in pairs) arise in many settings, and underpin a vast range of phenomena. In the context of quantum optics and information, they are known as parametric amplifier interactions, and are a basic resource for generating squeezing and entanglement [1, 2]; they also form the basis of quantum limited amplifiers [3]. In condensed matter settings, bosonic pairing underlies the theory of antiferromagnetic spin waves, interacting Bose-condensates, and can also be used to realize novel topological band structures [4, 5].

Given the importance of bosonic pairing, it is interesting to explore the basics of purely *dissipative* (or non-Hermitian) bosonic pairing. Non-Hermitian dynamics have garnered attention in a wide range of fields, from condensed matter [6–8] to optics [9–11] to classical dynamical systems [12–14]. In this Letter, we provide a comprehensive analysis of dissipative bosonic pairing in a fully quantum setting, showing it possesses a number of surprising and potentially useful features. We focus on minimal, experimentally realizable models, where bosons (e.g. photons) hop on a lattice, in the presence of a single dissipative pairing interaction. Remarkably, we find that while the dissipative pairing interaction on its own yields fully stable dynamics, when combined with simple lattice hopping (which is also stable), one can have dynamical instability. Further, close to such an instability, the quantum steady state is perfectly pure, with a selected subset of modes having high densities and strong squeezing and/or entanglement correlations. The complete state purity up until the instability threshold is a clear distinction from more standard instabilities associated with Hermitian pairing terms. Dissipative pairing is also distinct from the well-studied situation where a system is driven with squeezed noise; in particular, driving a quadratic, particle-conserving system with squeezed noise can never generate instability, whereas this readily occurs with dissipative pairing.

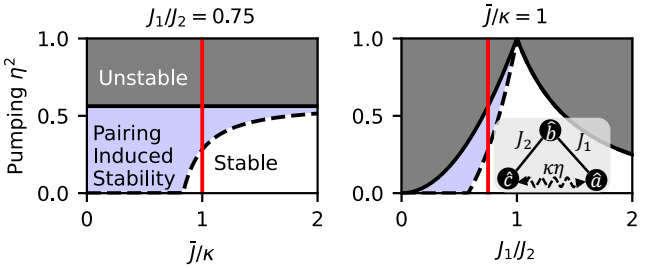

FIG. 1. Stability diagram for a minimal three-mode bosonic system (see inset) with loss on mode $\hat{a}$ (rate κ), gain on mode $\hat{c}$ (rate $\eta^2\kappa$), and tunnel couplings J_1, J_2 (c.f. Eq. (3)). In the absence of dissipative pairing, the system is dynamically unstable above the dashed line. Adding dissipative pairing $i\eta\kappa(\hat{a}\hat{c} + h.c)$ shifts the onset of instability to the solid line, see Eq. (4). Remarkably, this boundary is independent of $\overline{J}/\kappa$, where $\overline{J} = \sqrt{J_1^2 + J_2^2}$. The dissipative steady state remains pure (with a high density) as one approaches instability, see main text. Red lines in each plot are the same cut of parameter space, $\overline{J}/\kappa = 1.5$ and $J_1/J_2 = 0.75$. Solid lines show hopping, dashed line shows the dissipative pairing interaction.

Dissipative pairing becomes even more interesting when combined with topological bandstructures. We find that our new pairing instabilities are highly susceptible to wavefunction localization of the underlying lattice Hamiltonian. Hence, if the lattice supports exponentially-localized topological edge modes, we are able to selectivity excite and entangle them. Such topological systems remain a cornerstone of condensed matter physics [15–17] and photonics [18–20], and selectively exciting edge modes has been the subject of a flurry of recent proposals [21–26]. These are motivated by applications including

topological lasing [23, 26–29] and topological amplification and squeezing [24, 30–32]. However, these proposals often require complicated momentum and/or energy selectivity [24–26], as well as control over the entire lattice, [24–26, 30]. Here, we are able to get edge-mode selectivity almost for free, using a single quasi-local dissipative interaction.

Minimal model.—We start with a three-mode system (bosonic annihilation operators $\hat{a}, \hat{b}, \hat{c}$) that exhibits much of the surprising physics of interest. The key ingredient will be a dissipative pairing interaction between $\hat{a}$ and $\hat{c}$, that is an interaction generating dynamics of the form $\partial_t\langle\hat{a}\rangle = -\lambda\langle\hat{c}^\dagger\rangle$ and $\partial_t\langle\hat{c}^\dagger\rangle = \lambda^*\langle\hat{a}\rangle$. Because of the relative sign here, this dynamics *cannot* be obtained from a Hermitian pairing interaction. Instead, it would seem to correspond to a non-Hermitian effective Hamiltonian:

$$\hat{\mathcal{H}}_{\text{pairing}} = -i(\lambda\hat{a}^\dagger\hat{c}^\dagger + h.c.). \tag{1}$$

To obtain this Markovian dissipative dynamics in a fully quantum setting, this dissipative interaction must necessarily be accompanied by noise as well as local damping and anti-damping [7, 33]. The resulting description has the form of a Lindblad master equation [34, 35]. Using a minimal noise realization of the interaction, and letting $\hat{\rho}$ denote the system density matrix, we obtain

$$\dot{\hat{\rho}} = \hat{L}\hat{\rho}\hat{L}^\dagger - \left\{\frac{\hat{L}^\dagger\hat{L}}{2}, \hat{\rho}\right\} \equiv \mathcal{D}[\hat{L}]\hat{\rho}, \quad \hat{L} = \sqrt{\kappa}\hat{a} + \eta\sqrt{\kappa}\hat{c}^\dagger. \tag{2}$$

This purely dissipative evolution generates local damping on $\hat{a}$ with strength κ, local anti-damping on $\hat{c}$ with strength $\eta^2\kappa$, and a dissipative interaction of the form of Eq. (1) with $\lambda = \eta\kappa/2$. We take $\eta < 1$ (i.e. more local damping than anti-damping), which ensures dynamical stability (i.e. no tendancy for exponential growth) [36].

The dissipation in Eq. (2) is reminiscent of the dynamics generated by driving modes $\hat{a}$, $\hat{c}$ with broadband two-mode squeezed (TMS) noise [37]. There are however crucial differences. Driving with TMS noise always generates two dissipators; to make Eq. (2) equivalent to injected TMS, we would thus have to add the additional dissipator $\mathcal{D}[\sqrt{\kappa}\hat{c} + \eta\sqrt{\kappa}\hat{a}^\dagger]$. This complementary dissipator would completely cancel the effective dissipative interaction between a and c generated by $\mathcal{D}[\hat{L}]$, leaving only driving with correlated noise. There would thus be no interaction from the dissipation in the equations of motion between $\langle\hat{a}(t)\rangle$ and $\langle\hat{c}^\dagger(t)\rangle$. In contrast, we will show that in Eq. (2), the direct dissipative interaction between modes $\hat{a}$ and $\hat{c}$ plays a crucial role.

To see explicitly that dissipative pairing is distinct from input TMS, we will add coherent hopping interactions to our system, and consider the evolution of average values. The hopping is described by $\hat{\mathcal{H}} = J_1\hat{a}^\dagger\hat{b} + J_2\hat{b}^\dagger\hat{c} + h.c$, with the evolution now given by $\partial_t\hat{\rho} = -i[\hat{\mathcal{H}}, \hat{\rho}] + \mathcal{D}[\hat{L}]\hat{\rho}$. Because of linearity, the equations of motion for averages of mode operators are insensitive to noise, and only influenced by interactions (coherent and dissipative). For our system, a symmetry argument [36] lets us reduce the dynamics of these averages to the closed linear dynamics of the quadratures $\vec{v} = (x_a, p_b, x_c)$, where $\langle\hat{a}\rangle = (x_a + ip_a)/\sqrt{2}$, etc; the orthogonal quadratures (p_a, x_b, p_c) have an analogous closed evolution. We find $\partial_t\vec{v} = -iD\vec{v}$, where the dynamical matrix $D = D_J + D_\kappa$ can be interpreted as an effective 3×3 Hamiltonian matrix, and

$$D_J = \begin{pmatrix} 0 & iJ_1 & 0 \\ -iJ_1 & 0 & -iJ_2 \\ 0 & iJ_2 & 0 \end{pmatrix}, \; D_\kappa = \frac{\kappa}{2}\begin{pmatrix} -i & 0 & -i\eta \\ 0 & 0 & 0 \\ i\eta & 0 & i\eta^2 \end{pmatrix}. \tag{3}$$

The off-diagonal $\pm i\eta\frac{\kappa}{2}$ terms in D_κ are the dissipative interaction, which surprisingly adds a *Hermitian* contribution at the level of the dynamical matrix. This mirrors the fact that had we started with a non-dissipative Hermitian pairing interaction, we would generate a *non-Hermitian* dynamical matrix [38]. Note that the hopping dynamics on its own generates stable dynamics, as does the dissipative dynamics on its own. More formally, both the matrices D_J and D_κ have no eigenvalues with positive imaginary part and hence are dynamically stable (in the Lyapunov sense [39] that there is no tendency for exponential growth).

We now come to our first surprise: while each part of our dynamics (hopping, dissipation) is stable individually, combining them can lead to instability. We find that for the full dynamics, whenever $J_1 \neq J_2$, there will be a critical value of η beyond which we have exponential growth. Specifically, one can show [36] that the dynamical matrix in Eq. (3) will be unstable if

$$\eta > \min\left(|J_1/J_2|, |J_2/J_1|\right). \tag{4}$$

We stress that this phenomenon is distinct from recently studied "dissipation-induced instabilities" [40], where the purely dissipative dynamics is already unstable on its own. Again, in our case the system is always stable in the dissipation-only limit $J_1 = J_2 = 0$.

The instability threshold Eq. (4) can be understood from a simple perturbative argument that is formally valid only when $\kappa \ll J_1, J_2$ (akin to a Fermi's Golden Rule (FGR) calculation). If we define $|\psi_i\rangle (i = 1, 2, 3)$ to be the (non-degenerate) eigenvectors of D_J, and treat D_κ as a small perturbation on top of this, then to first order $|\psi_i\rangle$ has a relaxation rate:

$$\Gamma_i = -\text{Im}\langle\psi_i|D_\kappa|\psi_i\rangle. \tag{5}$$

If an eigenmode has more amplitude on $\hat{c}$ than $\hat{a}$, there will be a value of $\eta < 1$ at which Eq. (5) is negative. This corresponds exactly to the condition in Eq. (4), and

is easy to understand intuitively (i.e. the eigenmode sees more anti-damping than damping). Surprisingly, this simple FGR argument turns out to be exact to all orders in κ: Eq. (4) is not perturbative [36]. We stress that this is a non-obvious phenonmenon. For example, consider a modified model where we eliminate dissipative pairing by replacing $\mathcal{D}[\hat{L}] \to \mathcal{D}[\sqrt{\kappa}\hat{a}] + \mathcal{D}[\sqrt{\kappa}\eta\hat{c}^\dagger]$ in our master equation. We are left with just incoherent gain and loss. In this case, the instability threshold would depend sensitively on the value of κ, with the FGR prediction only valid for $\kappa \to 0$, see Fig. 1.

We thus see that even at the semiclassical level, the dissipative pairing interaction yields surprises: instability from the combination of two individually-stable dynamical processes, with a threshold that is independent of the overall dissipation scale. Note that the above phenomena could alternatively be described (in a squeezed frame) as the interplay of asymmetric loss and Hermitian pairing interacting (see [36] for details and application to 2-mode models).

Extension to quantum lattices.—We now explore dissipative pairing in general multi-mode lattice systems, focusing on the possibility of non-trivial dissipative steady states. Consider an N-site bosonic lattice, with annihilation operators $\hat{a}_i$ for each site. The coherent dynamics corresponds to a quadratic, number conserving Hamiltonian $\hat{\mathcal{H}} = \sum_{ij} H_{ij}\hat{a}_i^\dagger \hat{a}_j$. The only constraint we impose is that H possesses an involutory chiral sublattice symmetry U, such that $UHU^\dagger = -H$; our simple three-site model also had this symmetry. Chiral symmetry ensures that for every eigenmode of H with non-zero energy, there is a different eigenmode with an opposite energy.

We now add a single dissipative pairing interaction to the lattice, between two arbitrary sites $\overline{0}, \overline{1}$. Motivated by our three-mode example, we take $\overline{0}, \overline{1}$ to be on the same sublattice (as defined by the chiral symmetry). The full dynamics on the lattice is given by [41]

$$\partial_t \hat{\rho} = -i[\hat{\mathcal{H}}, \hat{\rho}] + \mathcal{D}[\hat{L}]\hat{\rho}, \quad \hat{L}/\sqrt{\kappa} = \hat{a}_{\overline{0}} + \eta \hat{a}_{\overline{1}}^\dagger. \tag{6}$$

Our goal is to understand instabilities and steady states of this setup. Note that previous work studied chiral-symmetric bosonic lattices driven by single-mode squeezing [42]. Such systems are completely distinct from our setup: they do not have any dissipative pairing interaction, never exhibit dynamical instability, and (unlike what we describe below) always yield steady states with a *spatially uniform* average density.

We start by diagonalizing $\hat{\mathcal{H}}$. Using chiral symmetry, we can write $\hat{\mathcal{H}} = \sum_{\alpha \geq 0} \epsilon_\alpha (\hat{d}_\alpha^\dagger \hat{d}_\alpha - \hat{d}_{-\alpha}^\dagger \hat{d}_{-\alpha})$. Eigenmode annihilation operators are given in terms of real space wavefunctions by $\hat{d}_{\pm\alpha} = \sum_i \psi_{\pm\alpha}[i]\hat{a}_i$. $\hat{\mathcal{H}}$ is invariant under two-mode squeezing transformations that mix a pair of $\pm\alpha$ modes [36]: for arbitrary $r_\alpha, \phi_\alpha \in \mathbb{R}$, if we take

$$\hat{\beta}_{\pm\alpha} \equiv \cosh(r_\alpha)\hat{d}_{\pm\alpha} + e^{i\phi_\alpha}\sinh(r_\alpha)\hat{d}_{\mp\alpha}^\dagger, \tag{7}$$

then $\hat{\mathcal{H}} = \sum_\alpha \epsilon_\alpha(\hat{\beta}_\alpha^\dagger \hat{\beta}_\alpha - \hat{\beta}_{-\alpha}^\dagger \hat{\beta}_{-\alpha})$.

We would like to find a set of r_α, ϕ_α such that:

$$\hat{L} = \sqrt{\kappa}\sum_\alpha N_\alpha(\hat{\beta}_\alpha + \hat{\beta}_{-\alpha}). \tag{8}$$

If this is possible, the system dynamics are stable, and we will have a unique steady state (vacuum of the $\hat{\beta}_{\pm\alpha}$ operators). Achieving Eq. (8) requires for each $\alpha > 0$ [36]:

$$\tanh r_\alpha = \eta \left| \frac{\psi_\alpha[\overline{1}]}{\psi_\alpha[\overline{0}]^*} \right|, \quad \phi_\alpha = \arg\left(\frac{\psi_\alpha[\overline{1}]}{\psi_\alpha[\overline{0}]^*} \right). \tag{9}$$

with $|N_\alpha|^2 = |\psi_\alpha[\overline{0}]|^2(1 - |\tanh r_\alpha|^2)$.

We now make a crucial observation: Eq. (9) only has a solution if $\eta < (|\psi_\alpha[\overline{0}]^*/\psi_\alpha[\overline{1}]| \equiv \eta_\alpha)$. If this condition is violated for a particular α, then the dynamics is unstable: in this case, we are forced to write $\hat{L}$ in terms of a Bogoliubov raising operator in the $(\alpha, -\alpha)$ sector, implying that the dissipation looks like anti-damping in this sector. At a heuristic level, for $\eta > \eta_\alpha$, the α modes see more gain than loss. Overall stability requires $\eta < \min \eta_\alpha \equiv \eta_c$, a condition that is independent of the dissipation strength κ. We thus have a generalization and rigorous justification of the surprising FGR-like instability condition in Eqs. (4) and (5) we found for the three-mode model.

Our arguments above imply that as long as $\eta < \eta_c$, we are dynamically stable and have a pure steady state, where each $(\alpha, -\alpha)$ pair is in a two-mode squeezed vacuum with a squeezing parameter given by Eq. (9). This will in general be a highly entangled state. Further, as $\eta \to \eta_c$ from below, the squeezing parameter of the critical modes is diverging, meaning that we will have a pure state where a small subset of modes contribute to a diverging photon number. Note this is very distinct from just incoherent gain and loss, which never has a pure steady state. This behaviour is also completely distinct from standard parametric instabilities, where the steady state becomes extremely impure as one approaches instability [43, 44]. The mode selectivity leads to a highly non-uniform density that can be exploited for applications, as we now discuss.

Dissipative pairing and topological edge states.— The physics discussed above is particularly striking when applied to chiral hopping Hamiltonians $\hat{\mathcal{H}}$ that have topological bandstructures. There are many such models, as chiral symmetry is a key part of the standard classification of topological bandstructures [45]. As our dissipative interaction always pairs opposite energy modes, edge modes will only be paired with edge modes, bulk modes only with bulk modes. Moreover, it is easy to ensure that the correlated steady-state photon density is concentrated on the edges. Edge-mode wavefunctions are exponentially damped in the bulk, so Eq. (9) tells us for

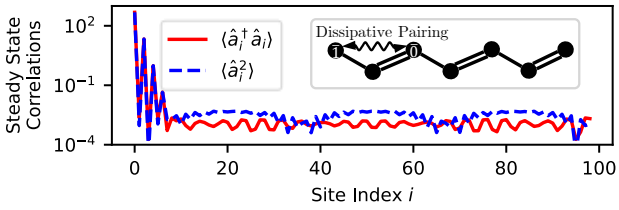

FIG. 2. Steady state correlation functions for a 99-site SSH chain with $\delta = -0.65$. There is a single jump operator of the form of Eq. (6) with $\overline{0} = 4$ and $\overline{1} = 0$, and $\eta = 0.999\eta_c \sim 0.045$. The squeezing correlation functions show a pure, single-mode squeezed state exponentially localized to the edge. Inset: Schematic of the dissipatively stabilized SSH chain. A single jump operator generates a dissipative pairing interaction, selectively exciting the edge mode.

an edge state α

$$\tanh r_\alpha = \eta \left| \frac{\psi_\alpha[\overline{1}]}{\psi_\alpha[\overline{0}]} \right| \propto \eta e^{(d_{\overline{0}} - d_{\overline{1}})/\zeta_L}, \tag{10}$$

where $d_{\overline{1},\overline{0}}$ is the distance from $\overline{1}$ and $\overline{0}$ to the edge, respectively, with ζ_L the localization length scale of the edge modes. If $d_{\overline{0}} - d_{\overline{1}} > 0$ (i.e. the gain site closer to the edge than the loss site), we obtain a super-exponential enhancement in the squeezing parameter of the edge modes. This yields large populations and squeezing on the edge (while still having a pure state), see Figs. 2 and 3.

For large enough systems, the bulk modes will be nearly translationally invariant, implying they will have $\tanh r_\alpha = \eta$. Thus, by spreading the two sites out over a few localization lengths ζ_L, a weak pump rate $\eta \ll 1$ can set $\tanh r_\alpha \sim 1$ for *only* the edge modes. Here, the total number of excitations in the bulk would be very small, $\langle \hat{n}_\alpha \rangle = O(\eta^2)$, whereas the number of excitations in the edge mode, as one approaches instability, will be super-exponentially enhanced and scales like: $\langle \hat{n}_\alpha \rangle = O([1 - \eta e^{(d_{\overline{0}} - d_{\overline{1}})/\zeta_L}]^{-1})$.

The upshot is that by using a single dissipative pairing interaction, we can selectively populate, squeeze and entangle edge modes of a topological bosonic band structure. Such states could be useful for applications in topological photonics [19], and are reminiscent of topological lasing states [23, 26] (which typically require complex schemes to only pump the edge states). We analyze this physics more carefully below for two prototypical topological hopping models (see Fig. 3).

SSH Chain.—A paradigmatic topological model is the SSH chain [46, 47], see Fig. 2 inset. This is a linear, 1D lattice with staggered hopping strengths, given by the Hamiltonian:

$$\hat{\mathcal{H}} = -J \sum_{i=1}^{N-1} (1 + (-1)^i \delta) \hat{a}_i^\dagger \hat{a}_{i+1} + h.c. \tag{11}$$

Such a model has been realized with bosons in a variety of experiments (e.g. [27–29, 48]). The topological regime

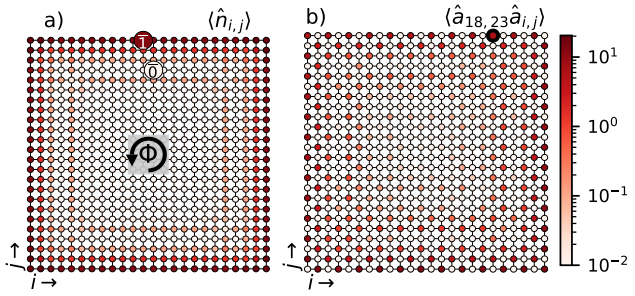

FIG. 3. (a) is a 24×24 site Hofstadter Lattice, which has uniform hopping and a quarter flux per plaquette $\Phi = \frac{1}{4}\Phi_0$. There is a single dissipator of the form of Eq. (6), with $\overline{1} = (11, 23)$ and $\overline{0} = (12, 20)$, and with $\eta = 0.999\eta_c \sim 0.0007$. The color corresponds to local steady state photon number, which is exponentially localized to the edges of the lattice. (b) is the same system, now showing steady state squeezing correlations between the randomly chosen edge site (18,23) and the rest of the lattice. Every edge site has exponentially enhanced squeezing with every other edge site on the same sublattice.

of $\hat{\mathcal{H}}$ admits one (two) protected edge modes if there are an odd (even) number of lattice sites, with a localization length $\zeta_L = (1 + \delta)/(1 - \delta)$. As $\alpha \to -1$, $\zeta_L \to 0$, and the edge modes become infinitely localized.

We consider for simplicity an odd number of lattice sites (see [36] for even N). This yields a single zero-energy edge mode, localized on a single sublattice. Hence, if we place the pairing dissipator on the correct sublattice, we can selectively excite just the edge mode into a single-mode squeezed vacuum with a super-exponentially enhanced squeezing parameter. The dissipative steady state for such a situation is plotted in Fig. 2. We thus have a resource-friendly approach for creating topologically-protected, bright non-classical squeezed light, using an SSH chain with a single, quasi-local, linear dissipator. One could imagine using the stabilized photons by weakly coupling the edge lattice site to an output waveguide, see [36] for more details. Note that topological features of the SSH chain are protected against disorder in the hopping coefficients up to the bulk gap $2|\delta|J$. We find that the qualitative nature of the dissipative steady state is also protected against hopping disorder over a similar scale (see [36]).

Hofstadter Lattice – 2D topological systems admit extended boundaries, allowing one to more easily study entanglement properties. Motivated by this, we consider a finite, quarter-flux Hofstadter lattice [49]. This corresponds to a square lattice with a quarter magnetic flux quanta per plaquette (see Fig. 3) giving the Hamiltonian:

$$\hat{\mathcal{H}} = \sum_{m,n} \hat{a}_{m,n}^\dagger \hat{a}_{m+1,n} + e^{i\pi m/2} \hat{a}_{m,n}^\dagger a_{m,n+1} + h.c., \tag{12}$$

which has been realized experimentally in Refs. [50–52].

This Hamiltonian supports exponentially localized

modes which propagate chirally around the edge [50, 51, 53, 54]. The fact that they are extended around the full edge is critical for generating long-range entanglement.

With the same prescription of adding a dissipative interaction of the form of Eq. (6) with $\overline{1}$ on the edge and $\overline{0}$ in the bulk, the steady state solution has exponentially localized edge photon density, with nearly all-to-all edge correlations, Fig. 3. For a fixed η, these sites will obey a volume-law scaling in entanglement entropy, [36], where maximally separated edge sites are now highly entangled, Fig. 3. Having all edge sites lie on the same topological boundary is crucial for this to occur [36].

In the limit that $\eta \to \eta_c$, the steady state will be dominated by the topological edge modes approaching instability. Treating the edge as a ring, we can label these by their momenta k; the steady state has all momenta k and $k+\pi$ in a TMS vacuum. Close enough to instability, a single momentum will dominate, generating uniform edge photon densities, see Fig. 3a, and a "checkerboard" of correlations, see Fig. 3b. The checkerboard is a result of the chiral symmetry, which admits only correlations within a sublattice. The values of the correlations and densities can be understood directly from Eq. (10), where $\langle \hat{n}_{i,j} \rangle \sim \sinh(r_k)^2$ and $\langle \hat{a}_{i,j} \hat{a}_{i',j'} \rangle \sim \sinh(r_k)\cosh(r_k)$ are super-exponentially enhanced compared to the bulk modes. This gives an arbitrary amount of entanglement between any two edge sites on the same sublattice as $\eta \to \eta_c$. This also means that for a relatively weak dimensionless pumping ($\eta < 10^{-3}$ in Fig. 3), the steady state can still have a large number of photons ($O(10^2)$ in Fig. 3), that is completely independent of the strength of the dissipation κ compared to the Hamiltonian.

Implementation– The basic master equation is naturally suited for any circuit- or cavity-QED experimental platform that can generate tunable couplings, along with an engineered lossy mode. Quantum systems that have been able to successfully create topological photonic or phononic lattices spans superconducting circuits [48, 52], micropillar polariton cavities [27], photonic cavities [55], photonic crystals [53], ring resonators [28, 29, 50, 51, 56], and optomechanics [57, 58]. In order to generate the requisite jump operator in Eq. (6), one can couple the dissipation sites to an auxilliary bosonic mode $\hat{b}$ with the interaction

$$\hat{\mathcal{H}}_I = g\hat{b}^\dagger(\hat{a}_{\overline{0}} + \eta\hat{a}^\dagger_{\overline{1}}) + h.c. \tag{13}$$

In the limit that the auxiliary mode $\hat{b}$ is very lossy with a loss rate $\kappa \gg g$, this gives the desired jump operator, with an effective strength $\Gamma = 4g^2/\kappa$, [59]. This allows one to easily engineer the desired reservoir with few additional resources.

Conclusions– We have demonstrated that dissipative pairing interactions lead to a previously unexplored class of instabilities in bosonic systems, where stable Hamiltonians and stable dissipation combine to give unstable dynamics. We have shown that these instabilities are incredibly sensitive to topological boundaries, providing a new mechanism to selectively excite topological edge modes without needing any momentum or frequency selectivity. Moreover, the steady state of the dynamics remains pure all the way up to the instability point, allowing one to populate the edge with an arbitrary number of zero-temperature excitations. Our ideas are compatible with a variety of different experimental platforms, and require few resources to implement.

Acknowledgements– This work is supported by the Air Force Office of Scientific Research under Grant No. FA9550-19-1-0362, and was partially supported by the University of Chicago Materials Research Science and Engineering Center, which is funded by the National Science Foundation under Grant No. DMR-1420709. AC also acknowledges support from the Simons Foundation through a Simons Investigator Award (Award No. 669487, AC).

[1] C. M. Caves and B. L. Schumaker, New formalism for two-photon quantum optics. i. quadrature phases and squeezed states, Phys. Rev. A **31**, 3068 (1985).
[2] C. C. Gerry, Dynamics of su(1,1) coherent states, Phys. Rev. A **31**, 2721 (1985).
[3] W. H. Louisell, A. Yariv, and A. E. Siegman, Quantum fluctuations and noise in parametric processes. i., Phys. Rev. **124**, 1646 (1961).
[4] R. Shindou, R. Matsumoto, S. Murakami, and J.-i. Ohe, Topological chiral magnonic edge mode in a magnonic crystal, Phys. Rev. B **87**, 174427 (2013).
[5] V. Peano, M. Houde, C. Brendel, F. Marquardt, and A. A. Clerk, Topological phase transitions and chiral inelastic transport induced by the squeezing of light, Nature Communications **7**, 10779 (2016).
[6] E. J. Bergholtz, J. C. Budich, and F. K. Kunst, Exceptional topology of non-hermitian systems, Rev. Mod. Phys. **93**, 015005 (2021).
[7] A. McDonald, R. Hanai, and A. A. Clerk, Nonequilibrium stationary states of quantum non-hermitian lattice models, Phys. Rev. B **105**, 064302 (2022).
[8] S. Lieu, Topological phases in the non-hermitian su-schrieffer-heeger model, Phys. Rev. B **97**, 045106 (2018).
[9] R. El-Ganainy, M. Khajavikhan, D. N. Christodoulides, and S. K. Ozdemir, The dawn of non-hermitian optics, Communications Physics **2**, 37 (2019).
[10] W. Chen, S. Kaya Özdemir, G. Zhao, J. Wiersig, and L. Yang, Exceptional points enhance sensing in an optical microcavity, Nature **548**, 192 (2017).
[11] H. Hodaei, A. U. Hassan, S. Wittek, H. Garcia-Gracia, R. El-Ganainy, D. N. Christodoulides, and M. Khajavikhan, Enhanced sensitivity at higher-order exceptional points, Nature **548**, 187 (2017).
[12] M. Fruchart, R. Hanai, P. B. Littlewood, and V. Vitelli, Non-reciprocal phase transitions, Nature **592**, 363 (2021).
[13] C. Scheibner, A. Souslov, D. Banerjee, P. Surówka, W. T. M. Irvine, and V. Vitelli, Odd elasticity, Nature

Physics **16**, 475 (2020).
[14] K. Sone, Y. Ashida, and T. Sagawa, Exceptional non-hermitian topological edge mode and its application to active matter, Nature Communications **11**, 5745 (2020).
[15] X.-L. Qi and S.-C. Zhang, Topological insulators and superconductors, Rev. Mod. Phys. **83**, 1057 (2011).
[16] M. Z. Hasan and C. L. Kane, Colloquium: Topological insulators, Rev. Mod. Phys. **82**, 3045 (2010).
[17] D. J. Thouless, M. Kohmoto, M. P. Nightingale, and M. den Nijs, Quantized hall conductance in a two-dimensional periodic potential, Phys. Rev. Lett. **49**, 405 (1982).
[18] Y. Ota, K. Takata, T. Ozawa, A. Amo, Z. Jia, B. Kante, M. Notomi, Y. Arakawa, and S. Iwamoto, Active topological photonics, Nanophotonics **9**, 547 (2020).
[19] T. Ozawa, H. M. Price, A. Amo, N. Goldman, M. Hafezi, L. Lu, M. C. Rechtsman, D. Schuster, J. Simon, O. Zilberberg, and I. Carusotto, Topological photonics, Rev. Mod. Phys. **91**, 015006 (2019).
[20] L. Lu, J. D. Joannopoulos, and M. Soljačić, Topological photonics, Nature Photonics **8**, 821 (2014).
[21] S. Mittal, E. A. Goldschmidt, and M. Hafezi, A topological source of quantum light, Nature **561**, 502 (2018).
[22] R. Barnett, Edge-state instabilities of bosons in a topological band, Phys. Rev. A **88**, 063631 (2013).
[23] B. Hu, Z. Zhang, H. Zhang, L. Zheng, W. Xiong, Z. Yue, X. Wang, J. Xu, Y. Cheng, X. Liu, and J. Christensen, Non-hermitian topological whispering gallery, Nature **597**, 655 (2021).
[24] V. Peano, M. Houde, F. Marquardt, and A. A. Clerk, Topological quantum fluctuations and traveling wave amplifiers, Phys. Rev. X **6**, 041026 (2016).
[25] G. Engelhardt, M. Benito, G. Platero, and T. Brandes, Topological instabilities in ac-driven bosonic systems, Phys. Rev. Lett. **117**, 045302 (2016).
[26] M. Seclì, T. Ozawa, M. Capone, and I. Carusotto, Spatial and spectral mode-selection effects in topological lasers with frequency-dependent gain, APL Photonics **6**, 050803 (2021).
[27] P. St-Jean, V. Goblot, E. Galopin, A. Lemaître, T. Ozawa, L. Le Gratiet, I. Sagnes, J. Bloch, and A. Amo, Lasing in topological edge states of a one-dimensionallattice, Nature Photonics **11**, 651 (2017).
[28] M. Parto, S. Wittek, H. Hodaei, G. Harari, M. A. Bandres, J. Ren, M. C. Rechtsman, M. Segev, D. N. Christodoulides, and M. Khajavikhan, Edge-mode lasing in 1d topological active arrays, Phys. Rev. Lett. **120**, 113901 (2018).
[29] H. Zhao, P. Miao, M. H. Teimourpour, S. Malzard, R. El-Ganainy, H. Schomerus, and L. Feng, Topological hybrid silicon microlasers, Nature Communications **9**, 981 (2018).
[30] D. Porras and S. Fernández-Lorenzo, Topological amplification in photonic lattices, Phys. Rev. Lett. **122**, 143901 (2019).
[31] J. Medina Dueñas, G. O'Ryan Pérez, C. Hermann-Avigliano, and L. E. F. Foa Torres, Quadrature protection of squeezed states in a one-dimensional photonic topological insulator, Quantum **5**, 526 (2021).
[32] C. C. Wanjura, M. Brunelli, and A. Nunnenkamp, Topological framework for directional amplification in driven-dissipative cavity arrays, Nature Communications **11**, 3149 (2020).
[33] H.-K. Lau and A. A. Clerk, Fundamental limits and non-reciprocal approaches in non-hermitian quantum sensing, Nature Communications **9**, 4320 (2018).
[34] G. Lindblad, On the generators of quantum dynamical semigroups, Communications in Mathematical Physics **48**, 119 (1976).
[35] V. Gorini, A. Kossakowski, and E. C. G. Sudarshan, Completely positive dynamical semigroups of nlevel systems, Journal of Mathematical Physics **17**, 821 (1976).
[36] See Supplementary Material.
[37] B. Kraus and J. I. Cirac, Discrete entanglement distribution with squeezed light, Phys. Rev. Lett. **92**, 013602 (2004).
[38] Y.-X. Wang and A. A. Clerk, Non-hermitian dynamics without dissipation in quantum systems, Phys. Rev. A **99**, 063834 (2019).
[39] M. W. Hirsch, S. Smale, and R. L. Devaney, *Differential equations, dynamical systems, and an introduction to chaos* (Academic press, 2012).
[40] N. Dogra, M. Landini, K. Kroeger, L. Hruby, T. Donner, and T. Esslinger, Dissipation-induced structural instability and chiral dynamics in a quantum gas, Science **366**, 1496 (2019).
[41] We note that an analogous master equation has been studied for spins and fermions [61]; however, because they have a finite dimensional Hilbert space, they never experience instability. This makes the physics studied here qualitatively different, as it relies heavily on the interplay between dissipative pairing, instability, and wavefunction localization. These are not present in a fermionic or spin system.
[42] Y. Yanay and A. A. Clerk, Reservoir engineering of bosonic lattices using chiral symmetry and localized dissipation, Phys. Rev. A **98**, 043615 (2018).
[43] C. Gerry and P. Knight, *Introductory quantum optics* (Cambridge University Press, 2005).
[44] D. F. Walls and G. Milburn, *Quantum Optics* (Springer, 2008).
[45] A. P. Schnyder, S. Ryu, A. Furusaki, and A. W. W. Ludwig, Classification of topological insulators and superconductors in three spatial dimensions, Phys. Rev. B **78**, 195125 (2008).
[46] W. P. Su, J. R. Schrieffer, and A. J. Heeger, Solitons in polyacetylene, Phys. Rev. Lett. **42**, 1698 (1979).
[47] W. P. Su, J. R. Schrieffer, and A. J. Heeger, Soliton excitations in polyacetylene, Phys. Rev. B **22**, 2099 (1980).
[48] E. Kim, X. Zhang, V. S. Ferreira, J. Banker, J. K. Iverson, A. Sipahigil, M. Bello, A. González-Tudela, M. Mirhosseini, and O. Painter, Quantum electrodynamics in a topological waveguide, Phys. Rev. X **11**, 011015 (2021).
[49] D. R. Hofstadter, Energy levels and wave functions of bloch electrons in rational and irrational magnetic fields, Phys. Rev. B **14**, 2239 (1976).
[50] M. Hafezi, E. A. Demler, M. D. Lukin, and J. M. Taylor, Robust optical delay lines with topological protection, Nature Physics **7**, 907 (2011).
[51] M. Hafezi, S. Mittal, J. Fan, A. Migdall, and J. M. Taylor, Imaging topological edge states in silicon photonics, Nature Photonics **7**, 1001 (2013).
[52] C. Owens, A. LaChapelle, B. Saxberg, B. M. Anderson, R. Ma, J. Simon, and D. I. Schuster, Quarter-flux hofstadter lattice in a qubit-compatible microwave cavity array, Phys. Rev. A **97**, 013818 (2018).
[53] Z. Wang, Y. Chong, J. D. Joannopoulos, and M. Soljačić,

Observation of unidirectional backscattering-immune topological electromagnetic states, Nature **461**, 772 (2009).

[54] The astute reader may be concerned that the chiral Altland-Zirnbauer class AIII is topologically trivial in 2D. However, the quarter-flux Hofstadter lattice is not gapped at half-filling, instead meeting at Dirac cones. The gaps at 1/4 and 3/4 filling have no chiral symmetry, and therefore are in class A and topological.

[55] Y. Gong, L. Guo, S. Wong, A. J. Bennett, and S. S. Oh, Tailoring topological edge states with photonic crystal nanobeam cavities, Scientific Reports **11**, 1055 (2021).

[56] D. Leykam and L. Yuan, Topological phases in ring resonators: recent progress and future prospects, Nanophotonics **9**, 4473 (2020).

[57] A. Youssefi, S. Kono, A. Bancora, M. Chegnizadeh, J. Pan, T. Vovk, and T. J. Kippenberg, Topological lattices realized in superconducting circuit optomechanics (2021), arXiv:2111.09133 [quant-ph].

[58] V. Peano, C. Brendel, M. Schmidt, and F. Marquardt, Topological phases of sound and light, Phys. Rev. X **5**, 031011 (2015).

[59] C. Gardiner and P. Zoller, *Quantum noise: a handbook of Markovian and non-Markovian quantum stochastic methods with applications to quantum optics*, Springer Series in Synergetics (Springer, Berlin, 2004).

[60] A. A. Clerk, M. H. Devoret, S. M. Girvin, F. Marquardt, and R. J. Schoelkopf, Introduction to quantum noise, measurement, and amplification, Rev. Mod. Phys. **82**, 1155 (2010).

[61] A. Pocklington, Y.-X. Wang, Y. Yanay, and A. A. Clerk, Stabilizing volume-law entangled states of fermions and qubits using local dissipation, Phys. Rev. B **105**, L140301 (2022).